

Formation of the Stellar System and the Central Gravitation-Potential Vessel of Galaxies

Keiichi Kodaira^{1,2,3}  and Veselina Kalinova¹

¹Max Planck Institute for Radioastronomy,
Auf dem Hügel 69, 53121 Bonn, Germany
email: kodaira_keiichi0815@soken.ac.jp

²National Astronomical Observatory of Japan,
Osawa2-21-1, Mitaka-shi, Tokyo, Japan PC 181-8588

³SOKENDAI, International Village
Hayama-machi, Miura-gun, Kanagawa-ken, Japan, PC 240-0193

Abstract. The formation of the global stellar system of galaxies are studied through the circular velocity curves of CALIFA nearby galaxies by sequencing the depth and size of the central gravitation-potential vessel and its dynamical mass, relative to the masses of the stellar system and of the parent halo, with the population or age parameters, to explore the dynamical characteristics of the dissipative contracting baryonic matter.

Keywords. galaxies: kinematics and dynamics, galaxies: structure, galaxies: evolution

1. Stellar mass, dynamical mass, and halo mass

The stellar systems of the present-day normal galaxies reside in the central part of the parent halos under dynamical influences of baryonic matter (stars, dust, gas, black hole) and dark matter, in the central gravitation-potential vessel (CGPV), which was deepened by the dissipative contraction of baryonic matter. The resolved field spectroscopic data of 231 nearby galaxies from CALIFA (Calar Alto Legacy Integral Field Area; [Sánchez et al. 2012](#)) survey were used to derive the circular velocity curve (CVC or $V_c(R)$; [Kalinova et al. 2017](#)), proxies of the dynamical mass within CGPV (M_{dyn} ; [Kalinova et al.](#), in prep.), and mass of the stellar system (M_* ; [Kalinova et al. 2021](#)). The $M_* - M_{dyn}$ relation (Fig. 1, left) shows bimodality, similar to the $M_* - M_{halo}$ relation (Fig. 1, right) after the stellar-to-halo relation of [Moster et al. \(2013\)](#). We find an empirical relationship between the dynamical mass and the mass of the parent halo,

$$\log M_{dyn} = 0.68 \log M_{halo} + 3.1 \quad (1.1)$$

which is mono-modal in contrast to other relations typically bimodal, a low-mass branch for young disk-type galaxies and a high-mass branch for aged ellipsoid-type galaxies with the mode-transition at $\log M_* \sim 10.7$ ($\log M_{dyn} \sim 11.1$, $\log M_{halo} \sim 12.3$), suggesting that M_{dyn} might be one of important parameters to inter-relate the galaxy and the parent halo.

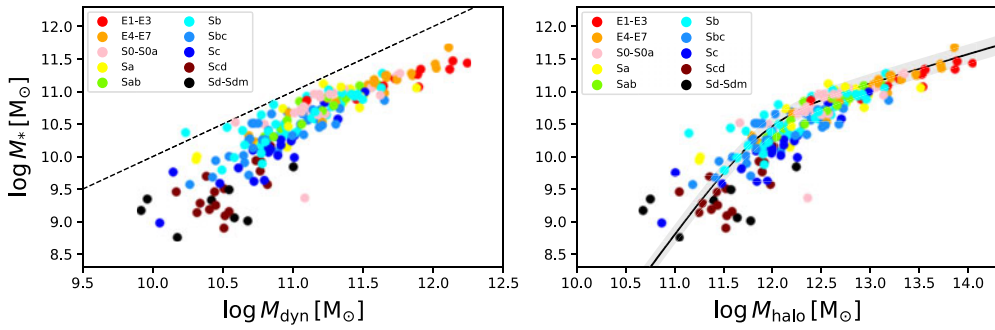


Figure 1. CALIFA-galaxy points are transferred from the M_* – M_{dyn} relation (left) to the M_* – M_{halo} relation (right) by applying the transformation of eq. 1.1, and fitted by the stellar-to-halo relation (black continuous line with an uncertainty grey band) of Moster et al. (2013). The dotted line in the left panel represents the one-one relation in the M_* – M_{dyn} plane, while the colour of the points indicate the morphological type of the galaxies.

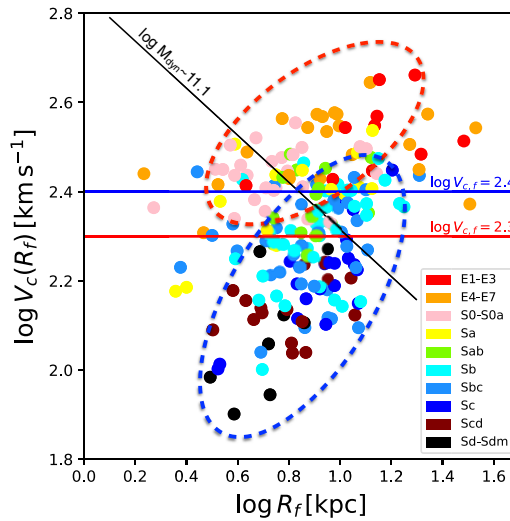


Figure 2. Amplitude versus size parameter diagram of the dynamical mass.

2. Bimodality and the dichotomy around the mode transition in the amplitude and size diagram of the CGPV

With CVC in hand, we introduce a proxy of the dynamical mass in the CGPV, $M_{dyn,f}$, with the standard analytical dependence on $\eta V^2(R/G)$ (V : velocity parameter, R : length parameter, G : gravitation constant, η : scaling factor);

$$\log M_{dyn,f} = 2 \log V_c(R_f) + \log R_f - \log G, \tag{2.1}$$

$R_f \equiv 1.5R_e$ (R_e – the effective radius of the galaxy), where the CVCs become flat and CALIFA velocity data are of high quality.

This proxy of the dynamical mass, $M_{dyn,f}$, is compared with the global dynamical mass M_{dyn} , to confirm the finding by Aquino-Ortiz et al. 2018 that all of the well devised dynamical-mass proxies can be regarded to be statistically the same, except for the scaling factor, η (in the present case $\eta \sim -0.15$). Taking the advantage of the analytical expression of $M_{dyn,f}$, we explore the nature of the bi-modality of the dynamical structure in terms of the potential-amplitude index, $V_c(R_f)$, and the size index, R_f (Fig. 2).

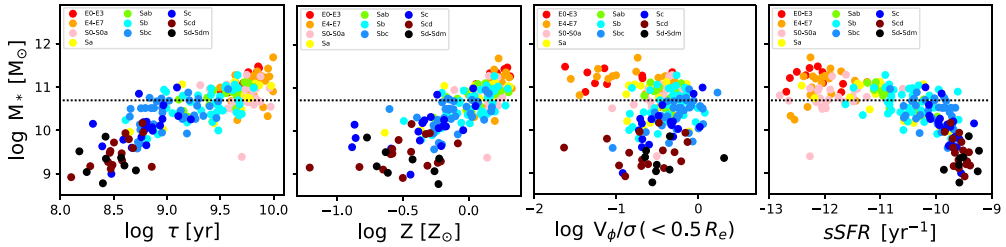


Figure 3. $\log M_*$ -sequence diagram (from left to right) of formation age ($\log \tau$), metallicity (Z), ordered-over-random motion (V_ϕ/σ) within $0.5 R_e$, and specific star-formation rate (sSFR). The horizontal line indicates the changing mode at $\log M_* \sim 10.7 M_\odot$.

The mode-transition is seen around $\log V_c(R_f) \sim 2.4$ (blue line), changing the dynamical structure from the disk-type to the ellipsoid-type. The transition of the dynamical structure occurs in the $M_* - M_{dyn}$ diagram (Fig. 1) around $\log M_{dyn} \sim 11.1$, which is indicated in Fig. 2 (black line), traversing the low-mass part of the red sequence and the highest-mass part of the blue sequence. The transition domain between the bimodal branches shows a kind of dichotomy, depending not only on the mass-concentration degree towards the center but also on the second parameter involving rotation characteristics to form the disk-system.

3. Characteristics of bimodal stellar systems and of the mode transition

In order to find any clues about the baryon-condensation history in CGPV, we examine the M_* -dependences of the population age τ , the heavy-element index Z , the ordered-over-random motion V_ϕ/σ in $R_e < 0.5$ (where V_ϕ is the azimuthal velocity and σ is the line-of-sight velocity), and the specific star-formation rate (sSFR) of the nearby CALIFA galaxies (Fig. 3) (parameter data are taken from Kalinova et al. 2017). Our findings are:

- (1) High-mass ($\log M_* > \sim 10.7$) spheroidal stellar systems (e.g. E0–E7) with dominant dispersion-motion were formed in early epochs, but later with poor baryon supply leading to no evident star-formation activity. They are embedded in correspondingly high-mass CGPVs ($\log M_{dyn} > \sim 11.1$) and high-mass halos ($\log M_{halo} > \sim 12.3$).
- (2) Low-mass ($\log M_* < \sim 10.7$) disk stellar systems (Sc–Sdm) with highly ordered rotational motion were formed in late epochs with continuous baryon supply to keep further star-formation activity. They are embedded in low-mass CGPVs ($\log M_{dyn} < \sim 11.1$) and in low-mass halos ($\log M_{halo} < \sim 12.3$). Among them, the CALIFA galaxies with the lowest mass ($\log M_* < \sim 9.7$, Scd–Sdm) are the youngest, and the star-formation activity is high in the shallow CGPVs, which might have resulted in the slight decrease of the V_ϕ/σ ratio.
- (3) The transition zone between the above two dominant dynamical types of stellar systems lies around $\log M_* \sim 10.7$ ($\log M_{dyn} \sim 11.1$, corresponding to $\log M_{halo} \sim 12.3$), where we notice a kind of dichotomy: On one side baryon is condensed into prominent (bulge + disk) stellar systems (e.g. Sab–Sbc) with strong ordered motion, while, on the other side at earlier epoch than the former, almost same amount of baryon condensed into the stellar systems with a dominant ellipsoidal/spheroidal component (e.g. S0–Sa), in which marginal-present gas-disks are prevented from active star formation, apparently due to the stabilizing gravitation-potential of the strong-concentrated stellar systems.

This mass-dependence study indicates that initial baryon infall in massive halos produced the central ellipsoidal stellar system whose dynamics/activity hindered succeeding in-fall of angular-momentum-rich baryonic matter to form the rotating disk, while in low-mass halos not enough low-angular-momentum baryon was available to form the dominant central ellipsoidal stellar system. These processes inevitably depend on the varying dynamical characteristics, in particular on the angular-momentum spectra, of the infalling baryonic matter of the parent halos, influenced by the merging/accretion prehistory. The present study suggests that massive halos tend to have more baryonic matter of low specific angular-momentum relative to low-mass halos.

References

- Moster, B. P., Naab, T., & White, S. D. M. 2013, *MNRAS*, 428, 3121
Sánchez, S. F., Kennicutt, R. C., Gil de Paz, A., et al. 2012, *A&A*, 538, A8
Aquino-Ortiz, E., Venzuela, O., Sánchez, S. F., et al., 2018, *MNRAS*, 479, 2
Kalinova, V., Colombo, D., Rosolowsky, E., et al., 2017, *MNRAS*, 469, 3
Kalinova, V., Colombo, D., Sánchez, S. F., et al., 2021, *A&A*, 648, A64